MIMO HSDPA Throughput Measurement Results in an Urban Scenario

Christian Mehlführer, Sebastian Caban, and Markus Rupp
Institute of Communications and Radio-Frequency Engineering, Vienna University of Technology
Email: {chmehl, scaban, mrupp}@nt.tuwien.ac.at; Web: http://www.nt.tuwien.ac.at/rapid-prototyping

***Abstract*—In this work, we report on results of MIMO High Speed Downlink Packet Access (HSDPA) throughput measurements. These measurements were carried out in an urban scenario. Besides the standard compliant SISO and two transmit antenna schemes, we defined and measured also a four antenna scheme. In all throughput measurements we used link adaptation, that is, adaptation of the channel coding rate and adaptive precoding. The measured throughput is compared to a so-called "achievable throughput" that is calculated based on the mutual information of the channel measured.**

I. Introduction

The High Speed Downlink Packet Access (HSDPA) mode [1] was introduced in Release 5 of UMTS to provide high data rates to mobile users. This is achieved by several techniques [2] like fast link adaptation [3], fast hybrid automated repeat request [4], and fast scheduling. In contrast to the pure transmit power adaptation performed in UMTS, fast link adaptation in HSDPA adjusts the data rate and the number of spreading codes depending on a so-called Channel Quality Indicator (CQI) feedback. MIMO HSDPA [5], recently standardized in Release 7 of UMTS, further increases the maximum downlink data rate by spatially multiplexing two independently coded and modulated data streams. Additionally, channel-adaptive spatial precoding is implemented at the basestation. The standard defines a set of precoding vectors of which one is chosen based on a so-called Precoding Control Indicator (PCI) feedback obtained from the user equipment.

In the past, a lot of research has been carried out to study various aspects of (MIMO) HSDPA, see for example [3–13] and the references therein. Among these studies, only a small number do not rely entirely on simulations but also deal with real world measurements [10–13]. None of them compares the actual data throughput of a (MIMO) HSDPA system with the mutual information and/or the capacity of the wireless channel. Motivated by this fact, we performed physical layer MIMO HSDPA throughput measurements. In this paper, we present results that were obtained in an extensive measurement campaign in the inner city of Vienna, Austria. Here, the propagation conditions are non-line-of-sight with a mean Root Mean Square (RMS) delay spread of 4.3 chips (corresponding to about 1.1 µs). We compare our throughput results to a so-called achievable throughput that is calculated using the mutual information of the channel. Additionally to the standardized 2×2 MIMO HSDPA system, we define and measure also a four transmit antenna HSDPA system to explore future enhancements of the standard.

The paper is organized as follows. In Section II, we provide an introduction to MIMO HSDPA and explain the precoding at the transmitter as well as the receiver processing. Section III gives a short overview about our measurement setup. Results are presented in Section IV. Finally, we conclude the paper in Section V.

II. MIMO HSDPA

In this section, we describe the (MIMO) HSDPA physical layer. In particular, we elaborate on the precoding at the transmitter, the channel modeling, and the equalization at the receiver. We restrict our analysis to slow fading; that is, we assume that the channel remains approximately constant during the transmission of one subframe (2 ms). A quasi-static channel is also a necessary condition for our measurements where we require a constant channel between the transmission of the "channel sounding"-block and the channel-adapted data block (see [14] for more details on our measurement approach). Furthermore, we assume that only one user per subframe is scheduled by the basestation.

A. System Model

Assume the transmission of N_s independently coded and modulated data chip streams, each of length $L_\mathrm{c} = L_\mathrm{h} + L_\mathrm{f} - 1$ chips; L_h corresponds to the channel length and L_f to the equalizer length. We define the stacked transmit chip vector $\mathbf{s}_k$ of length $N_\mathrm{s} L_\mathrm{c}$ at time instant k as

$$\mathbf{s}_k = \left[\mathbf{s}_k^{(1)\mathrm{T}}, \ldots, \mathbf{s}_k^{(N_\mathrm{s})\mathrm{T}}\right]^\mathrm{T}. \tag{1}$$

The N_s chip streams are weighted by the $N_\mathrm{T} \times N_\mathrm{s}$ dimensional precoding matrix

$$\mathbf{W} = \begin{bmatrix} w^{(1,1)} & \ldots & w^{(1,N_\mathrm{s})} \\ \vdots & \ddots & \vdots \\ w^{(N_\mathrm{T},1)} & \ldots & w^{(N_\mathrm{T},N_\mathrm{s})} \end{bmatrix} \tag{2}$$

forming the data chip streams of the N_T transmit antennas. At each transmit antenna, pilot, synchronization, and control channels accumulated in

$$\mathbf{p}_k = \left[\mathbf{p}_k^{(1)\mathrm{T}}, \ldots, \mathbf{p}_k^{(N_\mathrm{T})\mathrm{T}}\right]^\mathrm{T} \tag{3}$$

are added. Using the $L_c \times L_c$ dimensional identity matrix $\mathbf{I}_{L_c}$, the transmit signal vector $\mathbf{a}_k$ of length $N_T L_c$ is given by

$$\mathbf{a}_k = (\mathbf{W} \otimes \mathbf{I}_{L_c})\, \mathbf{s}_k + \mathbf{p}_k. \tag{4}$$

The frequency selective link between the n_t-th ($n_t = 1 \ldots N_T$) transmit and the n_r-th ($n_r = 1 \ldots N_R$) receive antenna is modeled by the $L_f \times L_c$ dimensional band matrix

$$\mathbf{H}^{(n_r,n_t)} = \begin{bmatrix} h_0^{(n_r,n_t)} & \cdots & h_{L_h-1}^{(n_r,n_t)} & 0 \\ \ddots & & \ddots & \\ 0 & h_0^{(n_r,n_t)} & \cdots & h_{L_h-1}^{(n_r,n_t)} \end{bmatrix}, \tag{5}$$

where the $h_i^{(n_r,n_t)}$ ($i = 0, \ldots, L_h - 1$) represent the channel impulse response between the n_t-th transmit and the n_r-th receive antenna. The entire frequency selective MIMO channel is modeled by a block matrix $\mathbf{H}$ consisting of $N_R \times N_T$ band matrices defined in (5)

$$\mathbf{H} = \begin{bmatrix} \mathbf{H}^{(1,1)} & \cdots & \mathbf{H}^{(1,N_T)} \\ \vdots & \ddots & \vdots \\ \mathbf{H}^{(N_R,1)} & \cdots & \mathbf{H}^{(N_R,N_T)} \end{bmatrix}. \tag{6}$$

At the receiver, the sum of noise and out-of-cell interference, denoted by $\mathbf{v}_k$, deteriorates the desired signal

$$\mathbf{b}_k = \mathbf{H}\mathbf{a}_k + \mathbf{v}_k = \mathbf{H}\,(\mathbf{W} \otimes \mathbf{I}_{L_c})\, \mathbf{s}_k + \mathbf{H}\mathbf{p}_k + \mathbf{v}_k. \tag{7}$$

The signal $\mathbf{b}_k$ is then processed in an equalizer $\mathbf{F}$ to obtain an estimate of the transmitted chip stream

$$\begin{aligned} \hat{\mathbf{s}}_k &= \left[\hat{s}_{k-\tau}^{(1)}, \ldots, \hat{s}_{k-\tau}^{(N_s)}\right]^T = \mathbf{F}\mathbf{b}_k \\ &= \mathbf{F}\mathbf{H}\,(\mathbf{W} \otimes \mathbf{I}_{L_c})\, \mathbf{s}_k + \mathbf{F}\mathbf{H}\mathbf{p}_k + \mathbf{F}\mathbf{v}_k. \end{aligned} \tag{8}$$

The equalizer matrix $\mathbf{F} = \left[\mathbf{f}^{(1)}, \ldots, \mathbf{f}^{(N_s)}\right]^T$ consists of N_s vectors $\mathbf{f}^{(n_s)}$, each of length $N_R L_f$.

B. Receiver

At the receiver, we first perform synchronization and iterative channel estimation according to [15]. After that, the interference of the deterministic signals, that is, the pilot and synchronization channels, is canceled. Therefore, in (8) the term $\mathbf{F}\mathbf{H}\mathbf{p}_k$ is reduced by $\mathbf{F}\hat{\mathbf{H}}\mathbf{p}_k$ and only interference caused by the channel estimation error $\left(\mathbf{H} - \hat{\mathbf{H}}\right)$ and the data channels remains. See [16] for a detailed post-equalization SINR analysis of such a receiver. Without interference cancelation, the post equalization SINR would saturate at about 20 dB, preventing error-free reception of larger CQI values [17, 18].

The equalizer coefficients are calculated in the minimum mean square error sense [19–21]. For the n_s-th data stream they are given as

$$\begin{aligned} \mathbf{f}^{(n_s)} = &\left(\mathbf{H}\left(\mathbf{W}\mathbf{W}^H \otimes \mathbf{I}_{L_c}\right)\mathbf{H}^H + \sigma_v^2 \mathbf{I}_{N_R L_c}\right) \cdot \\ &\cdot \mathbf{H}\,(\mathbf{W} \otimes \mathbf{I}_{L_c})\, \mathbf{e}_{\tau+(n_s-1)L_c}. \end{aligned} \tag{9}$$

Here, $\mathbf{e}_m$ denotes a unit vector with a "one" at position m and "zeros" at all other positions. Such equalizers are currently used in HSDPA receivers because they can be implemented efficiently using FFT-based algorithms like [22], or the conjugated gradient algorithm [23].

The output of the equalizer is soft-demapped and soft-decoded in a Turbo decoder using eight iterations. For the sake of completeness, we note that more complex MIMO receivers, like for example the LMMSE-MAP, are known to show about 1 dB better performance [24] than the standard LMMSE equalizer.

C. Quantized Precoding

The precoding matrix defined in (2) is strongly quantized and chosen from a predefined codebook in HSDPA systems [1]. For single antenna transmissions where obviously no spatial precoding can be performed, the precoding matrix $\mathbf{W}$ is reduced to a scalar equal to "one", thus $\mathbf{W}^{(\mathrm{SISO})} = 1$. For multiple antenna transmissions, the precoding matrices are composed of the scalars

$$w_0 = \frac{1}{\sqrt{2}} \tag{10}$$

and

$$w_1, w_2 \in \left\{ \frac{1+\mathrm{j}}{2}, \frac{1-\mathrm{j}}{2}, \frac{-1+\mathrm{j}}{2}, \frac{-1-\mathrm{j}}{2} \right\}. \tag{11}$$

The TxAA (Transmit Antenna Array) transmission mode utilizes two antennas to transmit a single stream. In this mode, the precoding matrix is defined as

$$\mathbf{W}^{(\mathrm{TxAA})} = \begin{bmatrix} w_0 \\ w_1 \end{bmatrix}. \tag{12}$$

This means that the signal at the first antenna is always weighted by the same scalar constant w_0, whereas the signal at the second antenna is weighted by w_1, chosen in order to maximize the received post equalization SINR [16]. In TxAA, the number of possible precoding matrices is equal to four, corresponding to an amount of 2 bit feedback.

In case of D-TxAA (Double Transmit Antenna Array) transmission, the precoding matrix is given by

$$\mathbf{W}^{(\mathrm{D-TxAA})} = \begin{bmatrix} w_0 & w_0 \\ w_1 & -w_1 \end{bmatrix}. \tag{13}$$

Note that this precoding matrix is a unitary matrix; that is, the precoding vector of the second stream is always chosen orthogonal to the one of the first stream. Although D-TxAA defines four precoding matrices, only the first two of them cause different SINRs at the receiver. In the other two cases, the SINRs of the first and the second stream are exchanged. Since the data rates of both streams can be individually adjusted, the third and the fourth precoding matrices are redundant.

The HSDPA standard does not define spatial precoding for four transmit antennas. Here we want to explore the benefits of four transmit antennas in HSDPA with a very simple extension of the existing precoding scheme. We define the precoding

Fig. 1. Panoramic view of the urban scenario measured (use PDF to zoom).

matrix for dual-stream four-antenna transmission as

$$\mathbf{W}^{(4\mathrm{Tx-D-TxAA})} = \begin{bmatrix} w_0 & 0 \\ 0 & w_0 \\ w_1 & 0 \\ 0 & w_2 \end{bmatrix}. \qquad (14)$$

In contrast to the two-antenna D-TxAA system, the four-antenna D-TxAA system now transmits the two data streams on individual antenna pairs. Also, the precoding of both streams is individually adjusted allowing 16 possible precoding matrices.

III. Measurement Set-Up

In the following, we briefly report on our measurement set-up in an urban scenario[1]. The measurement procedure is described in detail in [14], a testbed description is provided in [25].

The base-station antenna (Kathrein 800 10543 [26], $2\times\pm45°$ polarization, half-power beam width 58°/6.2°, down tilt 6°) was placed on the roof of a big building in the center of Vienna,Austria, 430 m away from the RX unit that was placed inside an office room, see Fig. 1. The base-station antenna is a so-called XX-Pol antenna that consists of two antenna pairs (A_1, A_2) and (A_3, A_4). These two antenna pairs are cross polarized and spatially separated by 1.24 wavelengths (15 cm). In case of transmissions which required two transmitter outputs, only one cross-polarized antenna pair (A_1, A_2) or (A_3, A_4) was utilized. When four transmitter outputs were required, the first data stream was transmitted with precoding on one polarization (A_1, A_3) and the second data stream on the other polarization (A_2, A_4). That is, each data stream was transmitted on the two, 1.24 wavelengths spatially separated, equally polarized antennas, either (A_1, A_3) or (A_2, A_4). Consequently, according to the definition of the precoding matrix in (14), the first two transmitter outputs were connected to the first antenna pair and the second two transmitter outputs to the second antenna pair.

At the RX unit we utilized four low-cost printed monopole antennas [27] which are based on the generalized Koch prefractal curve (for a photograph and the arrangement of the antennas see [28, Fig. 1]). Due to their low cost and small size, such antennas are very realistic and could be built into a mobile handset or a laptop computer. In all measurements carried out, the direct path from the TX to the RX antennas was blocked by the building the RX unit was located in. The channel in this scenario is characterized by a long mean RMS delay spread of 4.3 chips (corresponding to about 1.1 µs).

[1]Detailed transmitter and receiver positions can be downloaded for Google Earth at http://www.nt.tuwien.ac.at/fileadmin/data/testbed/Vienna-TX-RX-GPS.kmz.

IV. Measurement Results

In this section, we present the throughput measurement results (the solid lines in Fig. 2-3) and compare them to the "achievable throughput" (the dashed lines in Fig. 2-3). The achievable throughput is given by the channel capacity of a system that employs quantized precoding at the transmitter. A detailed definition of the achievable throughput is given in [29]. For all measurements, a Category 16 user equipment with a maximum throughput of 12.8 Mbit/s in single-stream and 28 Mbit/s in dual-stream mode is assumed.

All throughput curves presented in this section are plotted over total transmit power (measured at the inputs of the transmit antennas). Two additional x-axes show the average received SISO SNR and average received SISO signal power. The average received SISO signal power is obtained by averaging the received signal powers of all SISO transmissions, that is, the transmissions from every individual transmit antenna to every receive antenna. For a 4×4 MIMO system we thus average 16 SISO signal powers.

The reason why we plot the throughput over transmit power rather than SNR is the following: All MIMO schemes in HSDPA utilize adaptive precoding at the transmitter that effectively increases the received power and thus also the SNR while the total transmit power is the same as in the SISO transmission. If the throughput is plotted over SNR and not over transmit power, the curves will be shifted against each other. For example, in case of TxAA this shift would be about 2 dB compared to SISO. Therefore, all curves are plotted over transmit power. The additional x-axes (average received SISO SNR and average received SISO power) are only shown to indicate the approximate SNR and receive power ranges.

The precision of the measurement results was estimated by means of bootstrapping methods [30]. In all throughput graphs (Fig. 2-3), the dots represent the inferred mean throughputs, the vertical lines the corresponding 95% confidence interval, and the horizontal lines the corresponding 2.5% and 97.5% percentiles. Note that we did not change the RX antenna positions between measuring different schemes at different transmit power levels. This, on one hand, leads to smooth curves. On the other hand, the *relative* positions of the curves are far more accurate than the confidence intervals for the *absolute* positions might suggest.

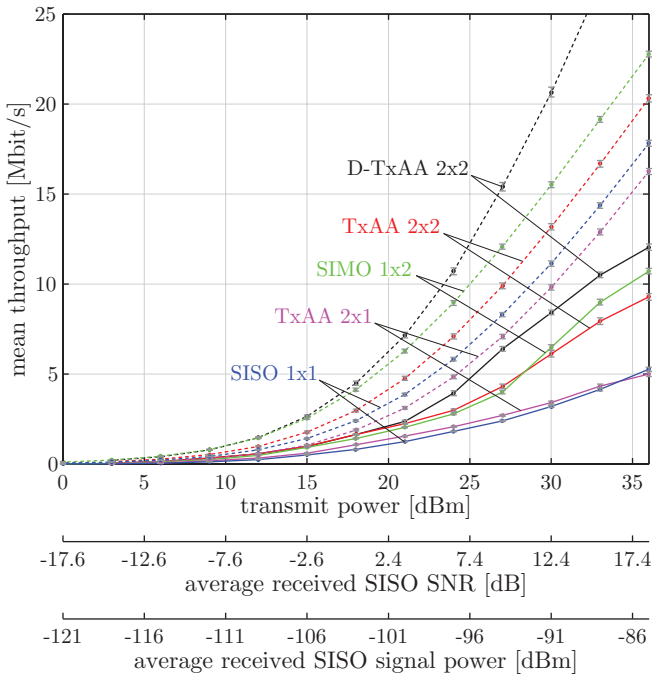

Fig. 2. Throughput results of the standard compliant schemes in the urban scenario (ID "2009-01-15c"). Averaging was performed over 484 receive antenna positions. The solid lines represent the measured throughput, the dashed lines the achievable throughput.

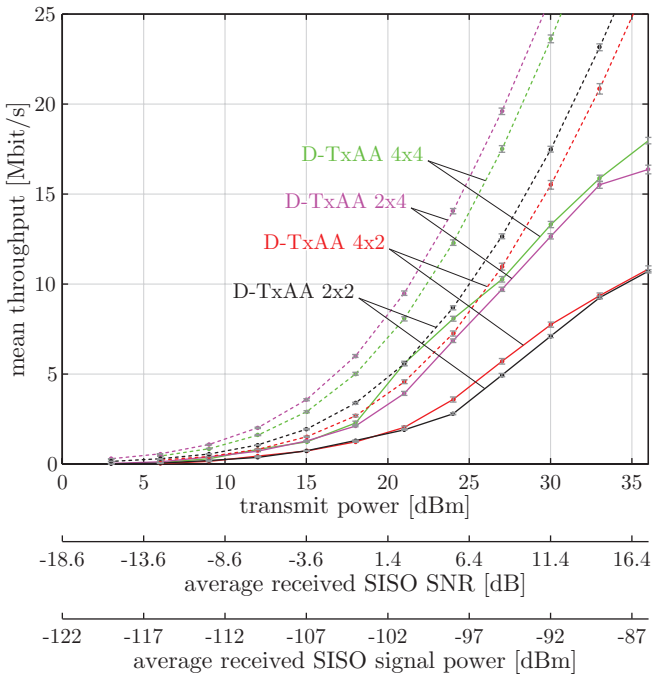

Fig. 3. Throughput results of the extended schemes in the urban scenario (ID "2008-12-12"). Averaging was performed over 484 receive antenna positions. The solid lines represent the measured throughput, the dashed lines the achievable throughput.

In Fig. 2, the results of the standard compliant schemes are shown. At low SNR, the 2×1 TxAA system only performs marginally better than the SISO system and worse than SISO at large SNRs. The reason for this is the rather large maximum delay spread of about 20 chips causing the precoding to be far from optimal. Optimal precoding has to be frequency depending (for example, water-filling solution). The large delay spread also causes inter-code interference that can only be partially removed by the MMSE equalizer.

The distance between the measured and the achievable throughput is evaluated at a transmit power of about 10-25 dBm to avoid saturation effects of the measured throughput. In this range, the SISO system looses about 9 dB in terms of SNR. Nevertheless, the 2×2 D-TxAA system yields about twice the throughput of the SISO system.

Fig. 3 shows the throughput of the four-antenna HSDPA schemes compared to the standard compliant 2×2 D-TxAA system. For the 4×4 system we measure about twice to three times the throughput of the 2×2 system. In terms of SNR, the 4×4 system gains about 9 dB over the 2×2 system. Comparing the achievable throughput [29] to the measured throughput reveals about 6 dB loss for the 2×2 system but only about 3 dB loss for the 4×4 system. Thus, the freedom of choosing a precoding matrix effectively allows to reduce the distance to the achievable throughput. It should be noted, though, that if optimum precoding were performed at the transmitter, the achievable throughput would be significantly larger.

Fig. 4 shows the measured throughput of all HSDPA schemes for transmit powers of 20 dBm and 30 dBm. The 4×4 scheme outperforms the SISO scheme by more than a factor of four and the 2×2 scheme by more than a factor of two.

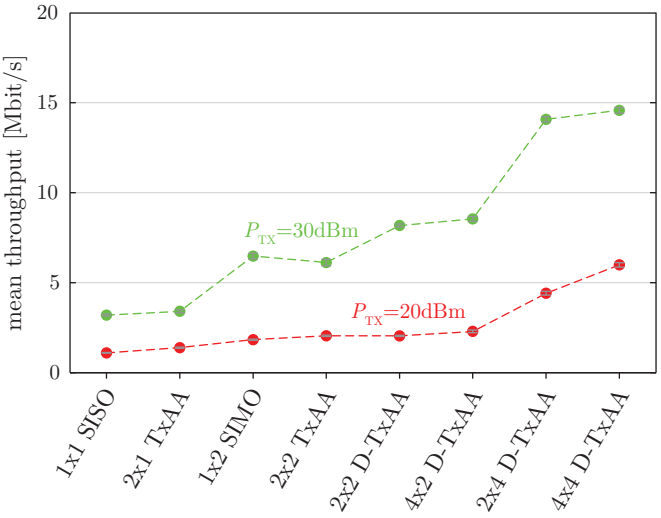

Fig. 4. Throughput increase of the different MIMO schemes for transmit powers $P_{TX} = 20$ dBm and $P_{TX} = 30$ dBm.

Thus, the extension of the existing MIMO HSDPA standard by a 4×4 scheme is attractive.

A. Discussion of the Throughput Loss

Although the results of the previous section show a significant performance increase of the different MIMO schemes when compared to the SISO transmission, a significant loss compared to the achievable throughput is observed. Several reasons cause this loss:

- The rate-matched Turbo code utilized in HSDPA is good but not optimal. At higher code rates, it looses up to 2 dB when decoded in a MAP decoder.

- The LMMSE equalizer representing a low complexity and cost-effective solution is also not optimal. Better receivers like the LMMSE-MAP have the potential to improve the performance by up to 1 dB [24].
- In case of MIMO transmission, the selection of a precoding matrix maximizing the post-equalization SINR decreases the loss to the achievable throughput.

V. Conclusions

MIMO HSDPA throughput measurement results obtained in a realistic urban scenario are presented in this paper. The campaign was carried out in the inner city of Vienna. The results show a considerable increase in the physical layer throughput when multiple antennas are employed at the transmit and the receive side. The standard compliant 2×2 system increases the physical layer throughput by more than a factor of two compared to the SISO system. The 4×4 system introduced furthermore increases the throughput by another factor of two. Comparing the measured to the achievable throughput (calculated based on the mutual information of the channel) shows that the measured throughput is far from optimal, loosing about nine decibels in SNR in case of SISO transmission but only three decibels in case of 4×4 MIMO transmission.

Acknowledgments

This work has been funded by the Christian Doppler Laboratory for Wireless Technologies for Sustainable Mobility, the Institute of Communications and Radio Frequency Engineering, and KATHREIN-Werke KG. The authors thank Constantine Kakoyiannis for providing the printed monopole RX antennas utilized in our measurements. The TX antennas were provided by KATHREIN-Werke KG. Also, the authors thank José Antonio García Naya, Michal Šimko, Walter Schüttengruber, and Georg Maier for supporting us with setting up the testbed.

References

[1] 3GPP, "Technical specification group radio access network; physical layer procedures (FDD) (Tech. Spec. 25.214 V7.7.0)," Nov. 2007.
http://www.3gpp.org/ftp/Specs/html-info/25214.htm

[2] T. E. Kolding, K. I. Pedersen, J. Wigard, F. Frederiksen, and P. E. Mogensen, "High speed downlink packet access: WCDMA evolution," *IEEE Vehicular Technology Society News*, pp. 4–10, Feb. 2003.
http://kom.aau.dk/group/05gr943/literature/hsdpa/evolution%20of%20HSDPA.pdf

[3] M. Nakamura, Y. Awad, and S. Vadgama, "Adaptive control of link adaptation for high speed downlink packet access (HSDPA) in W-CDMA," in *Proc. 5th International Symposium on Wireless Personal Multimedia Communications 2002*, vol. 2, Oct. 2002, pp. 382–386.
http://ieeexplore.ieee.org/stamp/stamp.jsp?arnumber=1088198

[4] A. Das, F. Khan, A. Sampath, and H.-J. Su, "Performance of hybrid ARQ for high speed downlink packet access in UMTS," in *Proc. 54th IEEE Vehicular Technology Conference 2001 (VTC2001-Fall)*, vol. 4, 2001, pp. 2133–2137.
http://ieeexplore.ieee.org/stamp/stamp.jsp?arnumber=957121

[5] H. Holma, A. Toskala, K. Ranta-aho, and J. Pirskanen, "High-speed packet access evolution in 3GPP release 7," *IEEE Communications Magazine*, vol. 45, no. 12, pp. 29–35, Dec. 2007.
http://ieeexplore.ieee.org/stamp/stamp.jsp?arnumber=4395362

[6] M. Assaad and D. Zeghlache, "On the capacity of HSDPA," in *Proc. 46th IEEE Global Telecommunications Conference 2003 (GLOBECOM 2003)*, vol. 1, Dec. 2003, pp. 60–64.
http://ieeexplore.ieee.org/stamp/stamp.jsp?arnumber=1258203

[7] T. Kolding, F. Frederiksen, and P. Mogensen, "Performance aspects of WCDMA systems with high speed downlink packet access (HSDPA)," in *Proc. 56th IEEE Vehicular Technology Conference 2002 (VTC2002-Fall)*, vol. 1, 2002, pp. 477–481.
http://ieeexplore.ieee.org/stamp/stamp.jsp?arnumber=1040389

[8] R. Love, A. Ghosh, R. Nikides, L. Jalloul, M. Cudak, and B. Classon, "High speed downlink packet access performance," in *Proc. 53rd IEEE Vehicular Technology Conference 2001 (VTC2001-Spring)*, vol. 3, 2001, pp. 2234–2238.
http://ieeexplore.ieee.org/stamp/stamp.jsp?arnumber=945093

[9] J.-B. Landre and A. Saadani, "Hsdpa 14,4 mbps mobiles - realistic throughputs evaluation," in *Proc. 67th IEEE Vehicular Technology Conference 2008 (VTC2008-Spring)*, May 2008, pp. 2086–2090.
http://ieeexplore.ieee.org/stamp/stamp.jsp?arnumber=4526024

[10] D. Samardzija, A. Lozano, and C. Papadias, "Experimental validation of MIMO multiuser detection for UMTS high-speed downlink packet access," in *Proc. 47th IEEE Global Telecommunications Conference 2004 (GLOBECOM 2004)*, vol. 6, Nov. 2004, pp. 3840–3844.
http://ieeexplore.ieee.org/stamp/stamp.jsp?arnumber=1379087

[11] M. Jurvansuu, J. Prokkola, M. Hanski, and P. Perala, "HSDPA performance in live networks," in *Proc. IEEE International Conference on Communications 2007 (ICC 2007)*, June 2007, pp. 467–471.
http://ieeexplore.ieee.org/stamp/stamp.jsp?arnumber=4288754

[12] T. Isotalo and J. Lempiainen, "HSDPA measurements for indoor DAS," in *Proc. 65th IEEE Vehicular Technology Conference 2007 (VTC2007-Spring)*, Apr. 2007, pp. 1127–1130.
http://ieeexplore.ieee.org/stamp/stamp.jsp?arnumber=4212667

[13] H. Holma and J. Reunanen, "3GPP release 5 HSDPA measurements," in *Proc. 17th IEEE International Symposium on Personal, Indoor and Mobile Radio Communications 2006 (PIMRC 2006)*, Sept. 2006.
http://ieeexplore.ieee.org/stamp/stamp.jsp?arnumber=4022310

[14] S. Caban, C. Mehlführer, G. Lechner, and M. Rupp, "Testbedding MIMO HSDPA and WiMAX," in *Proc. 70th IEEE Vehicular Technology Conference (VTC2009-Fall)*, Anchorage, AK, USA, Sept. 2009.

[15] C. Mehlführer and M. Rupp, "Novel tap-wise LMMSE channel estimation for MIMO W-CDMA," in *Proc. 51st IEEE Global Telecommunications Conference 2008 (GLOBECOM 2008)*, New Orleans, LA, USA, Nov. 2008.
http://publik.tuwien.ac.at/files/PubDat_169129.pdf

[16] C. Mehlführer, S. Caban, M. Wrulich, and M. Rupp, "Joint throughput optimized CQI and precoding weight calculation for MIMO HSDPA," in *Conference Record of the 42nd Asilomar Conference on Signals, Systems and Computers*, Pacific Grove, CA, USA, Oct. 2008.
http://publik.tuwien.ac.at/files/PubDat_167015.pdf

[17] M. Harteneck, M. Boloorian, S. Georgoulis, and R. Tanner, "Throughput measurements of HSDPA 14 Mbit/s terminal," *Electronics Letters*, vol. 41, no. 7, pp. 425–427, Mar. 2005.
http://ieeexplore.ieee.org/stamp/stamp.jsp?arnumber=1421242

[18] C. Mehlführer, S. Caban, and M. Rupp, "Measurement based evaluation of low complexity receivers for D-TxAA HSDPA," in *Proc. 16th European Signal Processing Conference (EUSIPCO 2008)*, Lausanne, Switzerland, Aug. 2008.
http://publik.tuwien.ac.at/files/PubDat_166132.pdf

[19] S. Geirhofer, C. Mehlführer, and M. Rupp, "Design and real-time measurement of HSDPA equalizers," in *Proc. 6th IEEE Workshop on Signal Processing Advances in Wireless Communications (SPAWC 2005)*, New York City, USA, June 2005, pp. 166–170.
http://publik.tuwien.ac.at/files/pub-et_9722.pdf

[20] L. Mailaender, "Linear MIMO equalization for CDMA downlink signals with code reuse," *IEEE Transactions on Wireless Communications*, vol. 4, no. 5, pp. 2423– 2434, Sept. 2005.
http://ieeexplore.ieee.org/iel5/7693/32683/01532226.pdf

[21] R. Love, K. Stewart, R. Bachu, and A. Ghosh, "MMSE equalization for UMTS HSDPA," in *Proc. 58th IEEE Vehicular Technology Conference 2003 (VTC2003-Fall)*, vol. 4, Oct. 2003, pp. 2416–2420.
http://ieeexplore.ieee.org/stamp/stamp.jsp?arnumber=1285963

[22] Y. Guo, J. Zhang, D. McCain, and J. R. Cavallaro, "An efficient circulant MIMO equalizer for CDMA downlink: Algorithm and VLSI architecture," *EURASIP Journal on Applied Signal Processing*, vol. 2006, Article ID 57134, 2006.
http://www.hindawi.com/GetPDF.aspx?doi=10.1155/ASP/2006/57134

[23] G. H. Golub and C. F. van Loan, Eds., *Matrix Computations*, 3rd ed. The Johns Hopkins University Press, 1996.

[24] J. Ylioinas, K. Hooli, K. Kiiskila, and M. Juntti, "Interference suppression in MIMO HSDPA communication," in *Proc. of the 6th Nordic Signal Processing Symposium 2004 (NORSIG 2004)*, 2004, pp. 228–231.
http://ieeexplore.ieee.org/stamp/stamp.jsp?arnumber=1344565

[25] S. Caban, C. Mehlführer, R. Langwieser, A. L. Scholtz, and M. Rupp, "Vienna MIMO testbed," *EURASIP Journal on Applied Signal Processing, Special Issue on Implementation Aspects and Testbeds for MIMO Systems*, vol. 2006, Article ID 54868, 2006.
http://publik.tuwien.ac.at/files/pub-et_10929.pdf

[26] Kathrein, "Technical specification Kathrein antenna type no. 800 10543."
http://www.kathrein.de/de/mcs/produkte/download/9363438.pdf

[27] C. Kakoyiannis, S. Troubouki, and P. Constantinou, "Design and implementation of printed multi-element antennas on wireless sensor nodes," in *Proc. 3rd International Symposium on Wireless Pervasive Computing 2008 (ISWPC 2008)*, Santorini, Greece, May 2008, pp. 224–228.
http://ieeexplore.ieee.org/stamp/stamp.jsp?arnumber=4556202

[28] J. A. García-Naya, C. Mehlführer, S. Caban, M. Rupp, and C. Luis, "Throughput-based antenna selection measurements," in *Proc. 70th IEEE Vehicular Technology Conference (VTC2009-Fall)*, Anchorage, AK, USA, Sept. 2009.

[29] C. Mehlführer, S. Caban, and M. Rupp, "MIMO HSDPA throughput measurement results," *IEEE Transactions on Vehicular Technology*, to be submitted.

[30] B. Efron and D. V. Hinkley, *An Introduction to the Bootstrap (CRC Monographs on Statistics & Applied Probability 57)*, 1st ed. Chapman & Hall, 1994.

Reference:

C. Mehlführer, S. Caban, and M. Rupp, "MIMO HSDPA Throughput Measurement Results in an Urban Scenario," in Proc. 70th IEEE Vehicular Technology Conference (VTC2009-Fall), Anchorage, AK, USA, Sept. 2009. [Online]. Available: http://publik.tuwien.ac.at/files/PubDat_176321.pdf

BibTeX:

```
@InProceedings{Mehlfuehrer_VTC2009f,
  author =        {Christian Mehlf\"uhrer and Sebastian Caban and Markus Rupp},
  title =         {{MIMO HSDPA} Throughput Measurement Results in an Urban Scenario},
  booktitle =     {Proc. 70th IEEE Vehicular Technology Conference (VTC2009-Fall)},
  month =         sep,
  year =          2009,
  address =       {Anchorage, AK, USA},
  url =           {http://publik.tuwien.ac.at/files/PubDat_176321.pdf},
}
```